
Exploring the Mechanisms of Dust Emission and Transport based on Observations and GEOS-Chem Simulations

Peili Zou¹, Xiaoyan Ma¹, Rong Tian², Jianqi Zhao¹, Tong Yang¹ and Yingying Ku¹

¹China Meteorological Administration Aerosol-Cloud and Precipitation Key Laboratory, Nanjing University of Information Science and Technology, Nanjing 210044, China

²Key Laboratory of Global Change and Marine Atmospheric Chemistry, Third Institute of Oceanography, Ministry of Natural Resources of China, Xiamen, China.

Correspondence: Xiaoyan Ma (xma@nuist.edu.cn)

Abstract:

Dust aerosols play a significant role in climate and air quality, yet understanding of their emission and long-range transport mechanisms remains incomplete. By looking into a severe dust event occurred in northern China on April 2025, and conducting the comparative analysis against a 30-year climatic average and the historical dust events using multi-source observations and the GEOS-Chem model simulations, we systematically investigate its meteorological conditions, emission mechanisms, and transport processes. Results show that the dust event in April was originated in the western Inner Mongolia (WIM) source region, accompanied by wind speeds exceeding 8 m/s and hourly PM₁₀ concentrations above 1900 $\mu\text{g}/\text{m}^3$, and affected the southern China including Yangtze River Basin and Hainan Province. Under the influence of the Siberian high-pressure system and the Mongolian cyclone, the WIM experienced persistent dry-cold advection (relative humidity around 20%, wind speeds exceeding 10 m/s). Three months preceding the dust event, the WIM exhibited significantly high temperatures ($\sim+2$ °C), reduced precipitation (~-25 mm) and low volumetric soil water (~-0.02 m³/m³). Comparison with two other severe historical dust events in year 2021 and 2023, demonstrating that long-range transport in 2025 was primarily due to strong northerly winds that effectively guided southward transport of dust aerosols-, which was mainly due to the sustained interaction between an intense Siberian High and a Mongolian cyclone, coupled with the southerly position of the cyclone. Furthermore, the dust in 2025 consistently moved southward but generally behind the rainband, which imply relatively low wet scavenging and thereby enabling stable long-range transport. The study confirms that persistent drought and strong winds triggered intense dust emission, and airflow transport under specific synoptic conditions dominated the long-range dust transport.

1 Introduction

Dust aerosols, which commonly originate from arid and semi-arid regions, significantly reduce visibility (Seinfeld et al., 2004; Tang et al., 2018), directly threat socioeconomic activities and public health (Griffin et al., 2004; Miri et al., 2022), alter regional climate through radiative effects (Twomey et al., 1977; Seinfeld et al., 2004), and by acting as ice nuclei modulate cloud microphysical processes and precipitation (Huang et al., 2006; Wang et al., 2010; Huang et al., 2014; Wang et al., 2015). Furthermore, dust-carried nutrients and pollutants can affect marine ecosystems, soil fertility, and vegetation growth, triggering complex ecological responses (Griffin et al., 2004; Wang et al., 2006; Gao et al., 2009; Gassó et al., 2010; Field et al., 2010). Observational studies indicate that dust aerosols emitted from East Asia can undergo long-range transport to Eastern China (Tan et al., 2012), Japan (Iwasaka et al., 1983), South Korea (Kim et al., 2008), and even North America (Guo et al., 2017), exerting multifaceted impacts on the climate, environment, and economy of these regions.

The Inner Mongolia Autonomous Region of China is one of the most important dust source regions in East Asia (Zhang et al., 2003; Tan et al., 2017). The underlying surface in its western part is primarily desert, while the central part is mainly grassland, providing favorable underlying surface conditions for the occurrence of dust events. Previous studies have indicated

that on longer time scales, the frequency of dust events in the Inner Mongolia region is primarily correlated with soil moisture and vegetation changes (Lee et al., 2011; Munkhtsetseg et al., 2016; An et al., 2018; Bao et al., 2021). The occurrence of dust weather normally relates to unstable atmosphere (Idso et al., 1976; Knippertz et al., 2006; Shao et al., 2020) and soil condition in dust source regions (Sun et al., 2001; Tegen et al., 2002). Most dust storms in the Inner Mongolia Autonomous Region occur mainly in spring, due to low vegetation coverage, scarce spring precipitation, and the influence of Mongolian cyclones (Gao et al., 2009; Liu et al., 2015; Borjigin et al., 2024), since strong winds associated with intense Mongolian cyclones create favorable dynamic conditions for the initiation and development of dust events (Takemi et al., 2005; An et al., 2018; Liu et al., 2024), and low vegetation coverage combined with minimal rainfall leads to dry and loose surface soil, providing ample material for dust emission.

The horizontal and vertical of dust transport depend on the meteorological conditions over the source region and the synoptic features in the downwind areas (Chen et al., 1987; McKendry et al., 2001), as well as the associated dry and wet deposition processes (Tsai et al., 2008; Liu et al., 2009; Fu et al., 2014; Chen et al., 2017). In dust source regions, the vertical transport of dust aerosols is primarily associated with turbulence and convection (Wang et al., 1990; Park et al., 2015; Richter et al., 2018). Brief bursts of turbulence facilitate the initial entrainment of dust into the atmosphere to become dust aerosols, while sustained turbulence promotes their vertical transport (Zhang et al., 2022). In the Asian Pacific Regional Aerosol Characterization Experiment (ACE-Asia), dust aerosols are typically lifted to approximately 3 km above the source region (Tsai et al., 2008). Under certain weather conditions, strong upward currents further elevate dust aerosols, thereby facilitating their long-range transport (Tsai et al., 2008). Long-range dust transport from Inner Mongolia relies on the dynamic forcing of northwesterly airflows. Previous studies indicated that under the influence of the Mongolian cyclone, northwesterly flows in the rear of upper-level troughs guide the dust aerosols from Mongolia and Inner Mongolia toward lower latitudes (Liu et al., 2009). Park et al. (2010) found dry deposition was approximately ten times greater than wet deposition near the source area, whereas wet deposition accounted for over 50% of the total in most downstream marine areas. Xiong et al. (2020) conducted a 20-year dust simulation and confirmed a significant seasonal variability in dust aerosol deposition over East Asia, with wet deposition consistently exceeding dry deposition in all months except December and January. Liang et al. (2022) analyzed an observed dust event in the Inner Mongolia Gobi Desert in March 2021 and found that wet deposition in the downwind North China Plain was approximately twice as effective as dry deposition.

In addition, the pathway and strengthens of dust long-range transport remains uncertain. Previous studies suggested that dust aerosols originating from Inner Mongolia primarily affect the North China Plain (Wang et al., 2004). For instance, during several typical dust events in March 2021, dust aerosols from northern China and southeastern Mongolia impacted regions including North China, southern Northeast China, and the northern Huang-Huai area (Yu et al., 2023). Dust aerosols from major Asian source regions (northern China and Mongolia) can be transported to southeastern Asia and the Pacific Ocean under the influence of westerly and southwesterly winds (Husar et al., 2001; Kai et al., 2007). Moreover, under specific meteorological conditions such as intense frontal cyclones, strong westerly jets, and limited precipitation-dominated wet deposition, dust aerosols from Mongolia and Inner Mongolia can undergo long-range transport to South Korea (Park et al., 2015), and Japan (Tsedendamba et al., 2019), and even North America (Zhao et al., 2008). The dust storm event occurred in western Inner Mongolia on April 11, 2025 is one of most severe dust events in recent years, which unusually penetrated southward across the Yangtze River Basin, eventually swept southwestern China and the South China Sea, so provides a comprehensive observations and opportunity for researchers to study dust-related processes. It is noteworthy that widespread precipitation occurred in the Yangtze River Basin during the transport of dust aerosols toward South China and Hainan Island. Under normal circumstances, such precipitation would significantly reduce aerosol concentrations through wet scavenging. However, in this event, the dust maintained relatively high concentrations and was still able to achieve ultra-long-range transport to Hainan Island. The mechanism behind this phenomenon of effective southward transport under strong wet

设置了格式: 字体颜色: 文字 1

[scavenging conditions warrants in-depth discussion.](#) This study integrates multi-source observational data with model simulations based on an improved GEOS-Chem model (Tian et al., 2020) to systematically analyze the dust emission characteristics, formation mechanisms, transport pathways, and the primary causes enabling the ultra-long-range transport of this dust event.

2 Data and measurements

2.1 Observational data

The hourly $PM_{2.5}$ and PM_{10} concentration provided by the China National Environmental Monitoring Center (<http://www.cnemc.cn/>) over 2,016 monitoring stations including 54 stations in western Inner Mongolia ($37^{\circ}N$ - $43^{\circ}N$, $98^{\circ}E$ - $112^{\circ}E$) (Figure 1a), and the daily Aerosol Optical Depth (AOD) at 550 nm from MODIS (Moderate-resolution Imaging Spectroradiometer)/Aqua Level 3 Dark Target Deep Blue Combined product (MOD08_M3, Collection 6.1) with $1^{\circ} \times 1^{\circ}$ spatial resolution, are employed to look into the dust events during the study period.

Meteorological variables such as near-surface wind speed, temperature, pressure, humidity, and precipitation, along with soil data, are obtained from the ECMWF ERA5 hourly reanalysis dataset from 1940 (<https://cds.climate.copernicus.eu/>), with a spatial resolution of $0.25^{\circ} \times 0.25^{\circ}$ and temporal resolution of one hour. These data are utilized to analyze the transport characteristics of dust aerosols, the synoptic conditions during dust events, and to conduct comparative analyses against both the 30-year climatological baseline and historical dust cases. Additionally, near-surface temperature and relative humidity from 2,167 meteorological stations (station distribution shown in Figure 1b) operated by the China Meteorological Administration (CMA, <http://data.cma.cn/>), with a temporal resolution of 3 hours, are used to evaluate the model performance. It is noteworthy that, due to the lack of precipitation observations from meteorological stations, ERA5 reanalysis data are used instead to assess the model's simulation of precipitation.

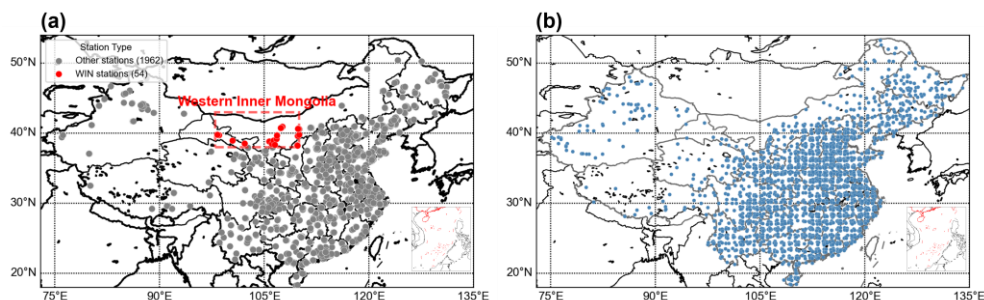


Figure 1. (a) Distribution of air quality monitoring stations in China. The area within the red rectangle ($38^{\circ}N$ - $43^{\circ}N$, $98^{\circ}E$ - $110^{\circ}E$) illustrates the distribution of stations in Western Inner Mongolia (WIM). Stations marked in red are located in WIM, while those in gray represent stations in other parts of China. (b) Distribution of Meteorological Stations in China. The small subplot in the lower right corner is the map of the Nine-Dash Line in the South China Sea.

2.2 Model description

The numerical simulations in this study were based on the GEOS-Chem model (<http://acmg.seas.harvard.edu/geos/>). As a global three-dimensional atmospheric chemical transport model, GEOS-Chem possesses the capability to simulate

atmospheric components from local to global scales and has been widely applied in various atmospheric composition studies.

This study used GEOS-Chem version 12.6.0, incorporating the dust emission scheme revised by Tian et al. (2020), which introduced spatially varying surface roughness lengths, updated soil property data, and physically based parameterizations of dust emission processes. These modifications enable the model to simulate threshold friction velocity and dust emission fluxes more accurately, reduce biases in simulated PM₁₀ concentrations and aerosol optical depth (AOD), and consequently better capture the spatiotemporal distribution characteristics of dust storms. (2020). The original dust emission scheme in GEOS-Chem is an empirical parameterization, in which the representation of many key physical quantities is highly simplified, particularly neglecting the spatiotemporal variations in surface conditions. This introduces substantial uncertainty into dust aerosol simulations. To better account for the effects of surface roughness elements and soil properties, Tian et al. (2020) replaced the originally assumed constant values with the actual spatial distributions of aerodynamic roughness length (α) and soil clay content (M_{clay}). Moreover, based on the global distribution of soil texture types, they improved the characterization algorithms for smooth-surface roughness length (z_{0s}) and the sandblasting efficiency α , endowing them with clearer physical meaning. Additionally, they incorporated the Owen effect and stress partitioning into the dust emission process. Simulation results show that optimizing the stress partitioning effect and the spatial distribution of surface roughness elements can significantly improve the simulation of the threshold friction velocity (u_{*t}). The improved scheme not only substantially reduces the original scheme's underestimation of PM₁₀ concentrations over China—lowering the normalized mean bias from -53% to -22%—but also more realistically reproduces the spatiotemporal variation characteristics of PM₁₀ concentrations in northern China, while simultaneously improving the simulation of aerosol optical depth (AOD).

The meteorological field data used in the model were obtained from the GEOS-FP reanalysis product provided by NASA's Global Modeling and Assimilation Office. The simulation period spanned from 00:30 UTC on April 8 to 11:30 UTC on April 15, 2025. The model configuration featured a horizontal resolution of 2°×2.5°, 72 vertical layers, a global simulation domain, and an output time interval of one hour.

3 A severe dust storm during 11~14 April, 2025 in Northern China

During April 2025 a severe dust storm swept across the most regions of China, from the Northern China to the Southern China. As one of the most severe dust storms in recent years, this dust event provides an excellent opportunity to study the related dynamical and physical on the dust processes.

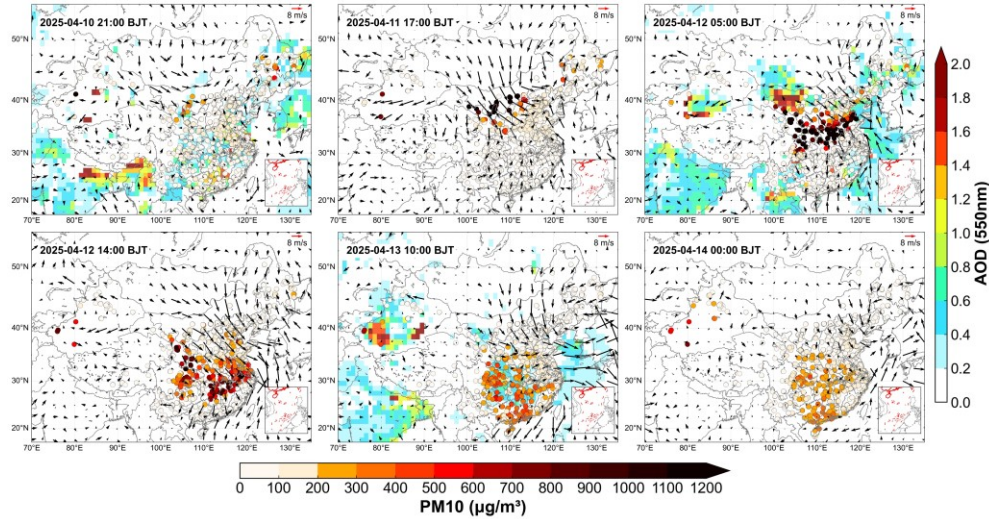
The PM₁₀ concentration monitored at surface and AOD from satellite retrievals are used here to represent the dust mass concentrations. The spatiotemporal variations of PM₁₀ and AOD, as well as wind fields during the dust periods are shown in Figure 2. It is evident that on April 10, both PM₁₀ and AOD in China remain quite low, with PM₁₀ concentrations below 200 $\mu\text{g}/\text{m}^3$ and AOD below 0.4 in most of China. The regionally-averaged PM₁₀, PM_{2.5}, and the ratio of PM_{2.5} to PM₁₀ in the WIM region (Figure 3) remains around 100 $\mu\text{g}/\text{m}^3$, 20 $\mu\text{g}/\text{m}^3$ and 0.3, and their ratio (PM_{2.5} to PM₁₀) showed a downward trend over time, respectively before 17:00 BJT (Beijing Time) on April 11th., decreasing from 0.4 at 06:00 on April 9 to 0.2 at 10:00 on April 11 (Figure 3). At 17:00 BJT on April 11th, a dust storm started to occur in WIM, accompanied by strong north winds over 8 m/s. It is noticed that the hourly PM₁₀ in WIM is greater than 1900 $\mu\text{g}/\text{m}^3$, while the ratio of PM_{2.5} to PM₁₀ dropped to approximately 0.2. The dust was rapidly transported southward, driven by strong northerly winds exceeding 10 m/s. During the subsequent 72 hours, the dust aerosols showed distinct spatiotemporal evolution, i.e. On April 12, the dust reached the Yangtze River Basin, where the PM₁₀ concentration exceeded 1000 $\mu\text{g}/\text{m}^3$ and the ratio of PM_{2.5} to PM₁₀ dropped below 0.2 (Figure 4). Meanwhile, the AOD in WIM exceeded 2 (Figure 2 and 4). By April 13, the dust arrived at Hainan Island, with the PM₁₀ concentration exceeding 300 $\mu\text{g}/\text{m}^3$ (Figure 2) and the ratio of PM_{2.5} to PM₁₀ being below 0.3 (Figure 4), marking the completion of long-range transport spanning 20 degrees of latitude. By April 14, the intensity of the dust had significantly weakened in the affected areas of Southeastern China, with PM₁₀ concentration mostly dropping below 300 $\mu\text{g}/\text{m}^3$, indicating

设置了格式: 字体颜色: 自动设置

设置了格式: 下标

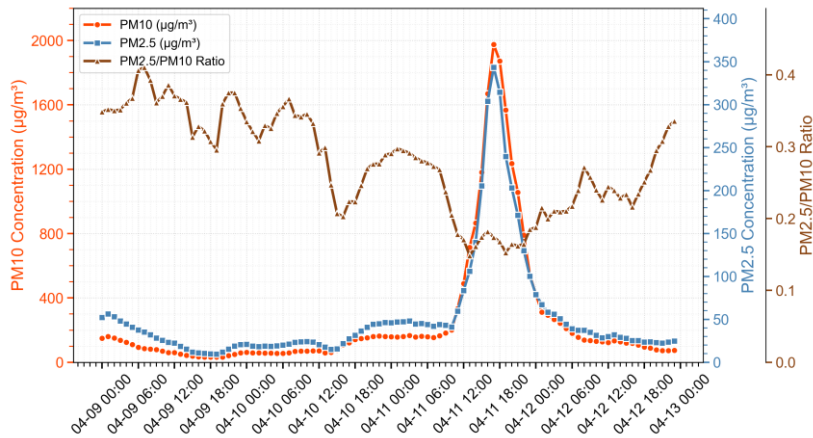
设置了格式: 字体颜色: 蓝色

the end of the dust event (Figure 2). In summary, this dust event, which originated in the WIM region on April 11 and concluded by April 14, significantly impacted a vast expanse of China through southward transport, affecting areas from the north and central to the southern parts of the country.



155

Figure 2. Spatiotemporal variations of PM_{10} concentration ($\mu g/m^3$) in China, AOD (MODIS) and surface wind fields (ERA5) over China and its surrounding areas from April 10 to 14, 2025 (BJT). The solid circles represent PM_{10} concentration, and the shaded plot represents AOD. The wind speed scale is located in the upper right corner of each panel, and the small subplot in the lower right corner is the map of the Nine-Dash Line in the South China Sea.



160

Figure 3. The hourly variations of PM_{10} , $PM_{2.5}$ concentrations ($\mu g/m^3$) and the $PM_{2.5}$ -to- PM_{10} ratio within the WIM region ($38^{\circ}N$ - $43^{\circ}N$, $98^{\circ}E$ - $110^{\circ}E$) during the dust events from April 9 to 12, 2025 (BJT).

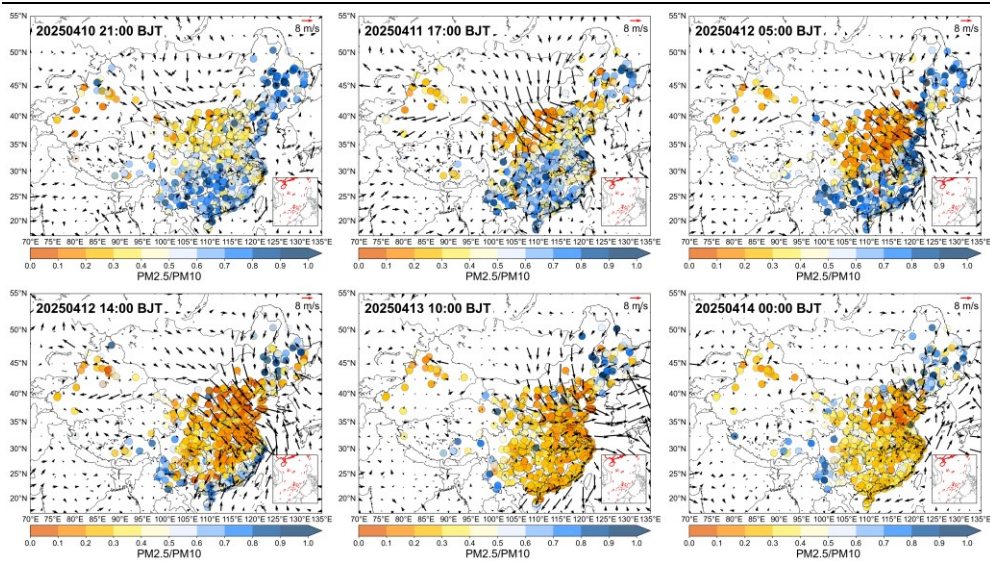


Figure 4. During April 10-14, 2025 (BJT), the spatiotemporal variations of $PM_{2.5}$ -to- PM_{10} ratio and surface wind fields (ERA5) over China.

It is known that the meteorological conditions including temperature, relative humidity, and wind fields significantly influence dust emissions and transport (Chepil et al., 1956; Zhang et al., 2002; Ravi et al., 2004; Hussein et al., 2006; Zhu et al., 2024; Wang et al., 2021). Temperature and humidity affect dust emissions by modulating soil moisture, surface friability, and vegetation coverage in source regions, while strong winds provide the necessary dynamic forcing for aerosol entrainment into the atmosphere and subsequent long-range transport (Zou et al., 2004; Liu et al., 2004; Xu et al., 2006; Guan et al., 2017). During transport, aerosols are primarily subject to dry and wet deposition (Bergametti et al., 2014). Dry deposition removes the aerosol particles from the atmosphere and toward the surface due to gravitational settling and turbulence or diffusion (Pryor et al., 2004; Bergametti et al., 2014; Ma and von salzen, 2006; Farmer et al., 2021). Wet deposition involves the incorporation of aerosols into hydrometeors (such as raindrops or cloud droplets), followed by their removal through precipitation (Zannetti et al., 1999; Pryor et al., 2004; Bergametti et al., 2014). Since turbulence intensity is often driven by thermal and mechanical energy (Roth et al., 2000; Hu et al., 2007), and droplet formation and fallout depend largely on precipitation, it is essential to consider meteorological factors when discussing aerosol transport.

4 Meteorological factors and dust processes

4.1 Synoptic processes

Previous studies found that large-scale circulation systems such as the polar vortex and the westerly jet influence the occurrence and transport of dust by affecting the development of the Mongolian cyclone and the southward movement of cold air masses, thereby regulating the upper-level jet stream and surface wind speeds (Zhao et al., 2004; Yang et al., 2008). In East Asia, Mongolian cyclones are the primary synoptic system responsible for most spring dust events (Li et al., 2022). More than 50% of the dust events occurring in Mongolia and northern China are solely triggered by Mongolian cyclones, while the remainder result from the combined influence of Mongolian cyclones and cold high-pressure systems (Borjigin et al., 2024).

For this dust event originating from the WIM region, particular attention should be paid to the role of the Mongolian cyclone and whether a cold Siberian high-pressure system is interacting with it. Figure 5 illustrates the evolution of synoptic conditions during the dust event from April 10 to 13, 2025. On April 10, eastern Outer Mongolia was influenced by a low-pressure system (central pressure was approximately 996 hPa), while the Mongolian cyclone had not yet fully developed. A Siberian high-pressure system (central pressure was exceeding 1028 hPa) was located along the northwestern border of Mongolia. Inner Mongolia was dominated by dry air mass (relative humidity around 30%) and influenced by cold northerly flow from Siberia, with westerly winds in the western region exceeding 10 m/s. By April 11, as the Siberian high (central pressure was exceeding 1036 hPa) moved southward to the northern border of Mongolia, the Mongolian cyclone formed over eastern Inner Mongolia with a central pressure below 996 hPa. The combined influence of these systems generated strong northerly winds exceeding 10 m/s, transporting dry, cold air southward. Relative humidity in Inner Mongolia dropped below 30%, with temperatures approaching 0°C. On April 12, the Mongolian cyclone migrated into northeastern China and intensified (central pressure near 996 hPa), while the Siberian high continued moving southward and weakened, with its central pressure dropping below 1030 hPa. Strong northerly winds persisted over Inner Mongolia and extended to the Yangtze River Basin, facilitating the southward transport of dry, cold air. The low-humidity center shifted to central China (relative humidity around 20%), and temperature in Inner Mongolia fell below 0°C. By April 13, the Mongolian cyclone further intensified, exhibiting a central pressure below 988 hPa. This development resulted in strong northeasterly winds dominating the southeastern coastal regions, which efficiently transported the dry, cold air mass from central China toward the South China Sea, causing relative humidity in southern China to decrease to 40%.

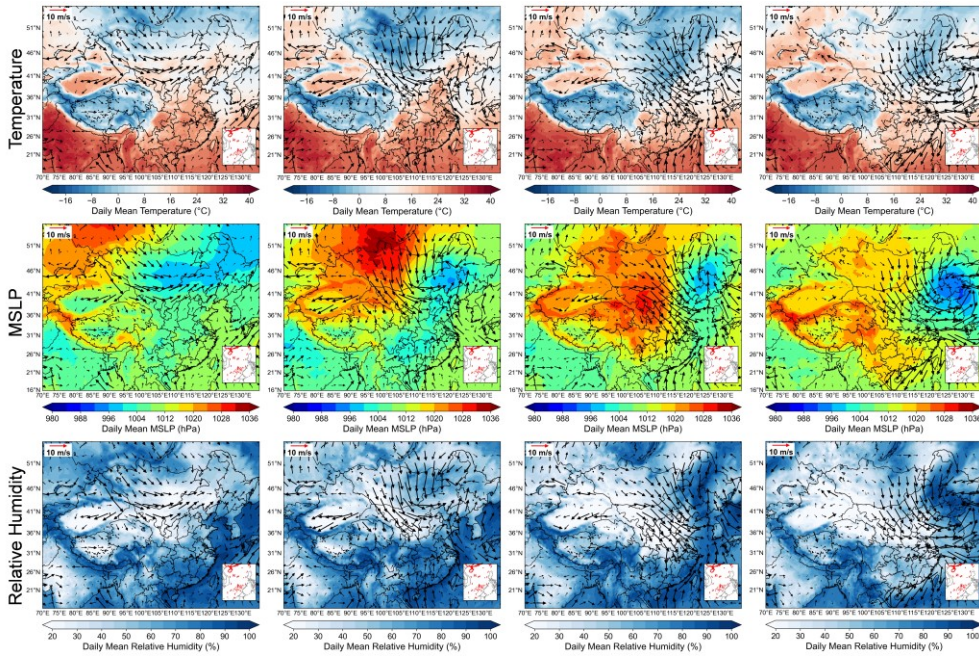


Figure 5. Spatiotemporal variations of daily mean temperature ($^{\circ}\text{C}$), mean sea level pressure (MSLP, unite: hPa), relative humidity (%), and [surface](#) wind fields over China from ERA5 during 10-13 April 2025 (BJT).

Throughout the event, WIM region remained under the influence of dry, cold air advection on the cyclone's western flank. The persistent occurrence of weather conditions characterized by low relative humidity and high wind speeds collectively created an optimal environment for dust transport. Meanwhile, the strong northerly winds generated by the synergistic effect of the Siberian high and Mongolian cyclone effectively transported dust toward the North China Plain (Figure 2). Additionally, the southward extension of dry, cold air masses reaching the Yangtze River Delta provided favorable conditions for the unusual long-range transport of dust to Hainan. In summary, the synergistic interaction between the Siberian high and the Mongolian cyclone served as the primary driving mechanism for this dust event, promoting the southward propagation of dry, cold air masses and enabling the long-range transport of dust aerosols.

4.2 Dust emission and transport

~~In order to facilitate a more comprehensive discussion of the characteristics of this dust event, model simulations were utilized to the analysis of the dust emission process. more comprehensively analyze the characteristics of this dust event, model simulations were employed to complement observational analysis, with a particular focus on the processes of dust emission and vertical transport. The available observational data can reveal the spatiotemporal distribution of dust concentrations, however, due to limited observational coverage—particularly the cessation of the CALIPSO satellite mission on 1 August 2023—it is difficult to fully resolve the event's detailed characteristics. Using the GEOS-Chem model, we were able to simulate dust emission fluxes and vertical transport under realistic meteorological conditions. This combined approach of observations and simulations enables a more complete depiction of the dust event's features and facilitates a better understanding of the mechanisms behind its unusual intensity and long-range transport.~~

The GEOS-Chem model employing a revised dust emission version by Tian et al. (2020), in which the geographical variation of aerodynamic roughness length, smooth roughness length and soil texture, the Owen effect, and the formulation of the sandblasting efficiency α by Lu and Shao (1999) are incorporated to improve dust emission over China. We performed a systematic model evaluation before utilizing model outputs for analysis of the dust event. The simulated meteorological conditions including temperature, relative humidity, precipitation, and wind fields during this dust event are evaluated against the observations on the weather stations and ERA5 reanalysis data. (Figure S1, S2), while the simulated dust mass concentrations are evaluated with observed PM₁₀ concentration, respectively (Figure S1, S2S3). Our evaluation indicated that the model effectively captured the key characteristics of meteorological fields and the spatiotemporal variations of dust aerosols during the April 2025 dust event. Specifically, from April 10 to 11, strong northerly winds (exceeding 8 m/s) dominated northern and central China. A dry-cold air mass intruded into the Inner Mongolia region on April 11, reducing relative humidity to below 30% and temperatures to near 0°C. High dust concentrations were located in western Inner Mongolia, with observed PM₁₀ levels surpassing 950 $\mu\text{g}/\text{m}^3$ and simulated dust aerosol concentrations exceeding 1000 $\mu\text{g}/\text{m}^3$, while precipitation was primarily concentrated in central China. Between April 12 and 13, the model continued to accurately capture the features of temperature, humidity, wind fields, and precipitation, as well as the general southward transport of dust aerosols. In a word, the model reproduced the southward movement of the dry-cold air mass, the transport of dust aerosols driven by northerly winds, and the concurrent southward shift of the precipitation.

Figure 6 shows the temporal variations of dust emission fluxes based on GEOS-Chem simulation. Relatively low dust emissions (less than 150 $\mu\text{g}/\text{m}^2/\text{s}$) were present in WIM region at 08:00 BJT on April 11, and dust emission fluxes exceeded 400 $\mu\text{g}/\text{m}^2/\text{s}$ by 16:00 BJT, after which the emissions weakened. It is known that both magnitude and direction of dust transport could be impacted by dust emission fluxes and its vertical distribution. CALIPSO satellite retrievals are widely used to examine the vertical profiles of aerosols including dust (Liu et al., 2008; Uno et al., 2008; Ma et al., 2013; Zhao et al., 2020; Chaibou et al., 2020). Unfortunately, such CALIPSO data are not available since August 1, 2023. In order to look into the vertical distribution of dust and its temporal variations, the simulated vertical distribution of dust mass concentrations along

设置了格式: 字体颜色: 自动设置

设置了格式: 字体颜色: 自动设置

设置了格式: 字体颜色: 自动设置

110°E at selected times from April 11 to 13 are presented (Figure 7). At 16:30 BJT on April 11, dust aerosols were concentrated between 35°N and 40°N, with vertical transport heights exceeding 3.6 km. Subsequently, the dust aerosols transported toward lower latitudes, reaching 30°N by 08:30 BJT on April 12, with transport heights decreasing to approximately 1.6 km. By 04:30 BJT on April 13, the dust aerosols had transported to regions below 25°N, with transport heights further declining to around 0.8 km. Combined with Figure 3, it can be observed that during this dust event, significant dust aerosol emissions occurred in WIM region at 16:30 BJT on April 11, indicating the onset of the dust emission process. The dust aerosols entered the atmosphere and were lifted to altitudes above 3.6 km under the influence of strong winds and other factors. By 17:00 BJT on April 11, the PM₁₀ concentration in WIM region sharply increased, reaching its peak value. Intense dust emissions provided abundant source materials for this dust event, while the lifting of dust aerosols over 3 km in the source region facilitated long-range transport (Idso et al., 1976; Tsai et al., 2008).

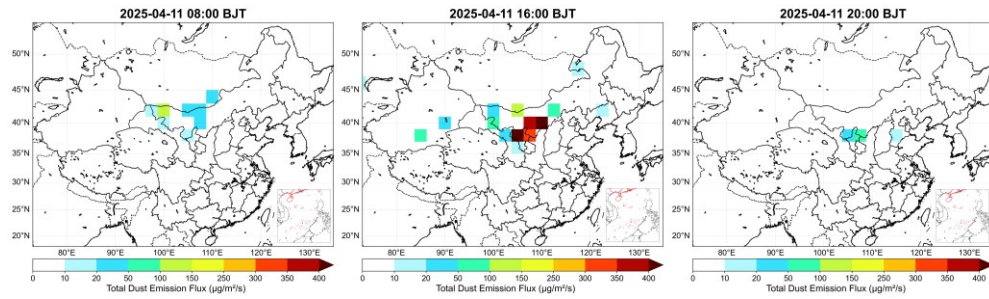


Figure 6. Spatial distribution of model-simulated dust emission fluxes ($\mu\text{g}/\text{m}^2/\text{s}$) on April 11, 2025 (BJT).

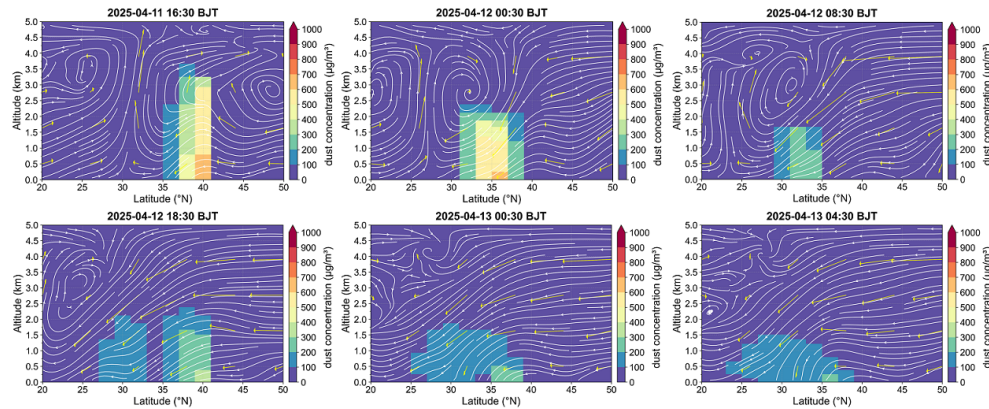


Figure 7. Vertical cross-section of dust concentrations ($\mu\text{g}/\text{m}^3$) along 110°E between 20°N and 50°N during 11-13 April 2025 (BJT), with simulated vertical-meridional wind streamlines.

4.3 Why is this dust storm so strong?

Previous studies found that the frequency of dust events in northern China has decreased in recent years, but the occurrence of severe dust storms has increased (Wang et al., 2018; Bao et al., 2021; Gavrouzou et al., 2021; Zhu et al., 2024). Earlier studies indicated that declining wind speeds, reduced precipitation, and increased vegetation coverage might contribute

带格式的：两端对齐，无，段落间距段前：0 磅，段后：0 磅

to the decrease in dust events across China (Guan et al., 2017; Wang et al., 2021). Prolonged drought, high temperatures, and short-term strong winds are key drivers of severe dust storms (Littmann et al., 1991; Attiya et al., 2020; Yong et al., 2021; Wang et al., 2022). The long-range transport of dust aerosols is primarily influenced by meteorological conditions in the source region and removal mechanisms during transport (Chen et al., 1987; Liu et al., 2009; Fu et al., 2014; Chen et al., 2017). In East Asia, precipitation-dominated wet deposition might play a more critical role than dry deposition in the long-range transport of dust aerosols (Zhao et al., 2003; Park et al., 2010; Liang et al., 2022). Therefore, it is essential to consider the long-term influences of humidity, precipitation and temperature, the short-term dynamic effects of wind speed, and the impact of precipitation-dominated wet deposition when analyzing the driving mechanisms and causes of long-range transport in this dust event.

4.3.1 Comparison of meteorological conditions with 30-year climatological mean

To understand the driving role of meteorological factors in this dust event, we analyzed the anomalies of temperature, volumetric soil water, and precipitation during the four months preceding the dust event. These meteorological anomalies are relative to the 30-year climatological baseline. The spatial distribution of temperature, volumetric soil water, and total precipitation anomalies from January 1, 2025, to April 14, 2025 (Figure 8a-c) indicates that relative to the 30-year climatological baseline, the WIM region (40-45°N, 95-105°E) exhibited higher-than-normal temperatures (Approximately +2 °C), lower-than-normal precipitation (Approximately -25 mm), and lower-than-normal volumetric soil water (Approximately -0.02 m³/m³) both during and for the three months preceding the dust event. Moreover, it is essential to focus on wind speed anomalies on shorter time scales immediately preceding the dust event. Figure 8d shows the daily mean wind speed anomalies in the WIM region from April 5 to 14, 2025. Approximately +2 m/s daily mean wind speed anomalies occurred before the dust outbreak (April 10), ~~and~~. Both the daily mean and daily maximum wind speed ~~anomaly anomalies~~ peaked (Approximately +2 m/s and +4m/s) on the day of the dust event (April 11). To summarize, compared to the climatological baseline, the WIM region experienced generally warm and dry conditions from January to April 2025, accompanied by pronounced short-term strong winds preceding the dust event. These factors served as critical drivers of this intense dust episode, providing the necessary material and dynamic conditions for dust emission.

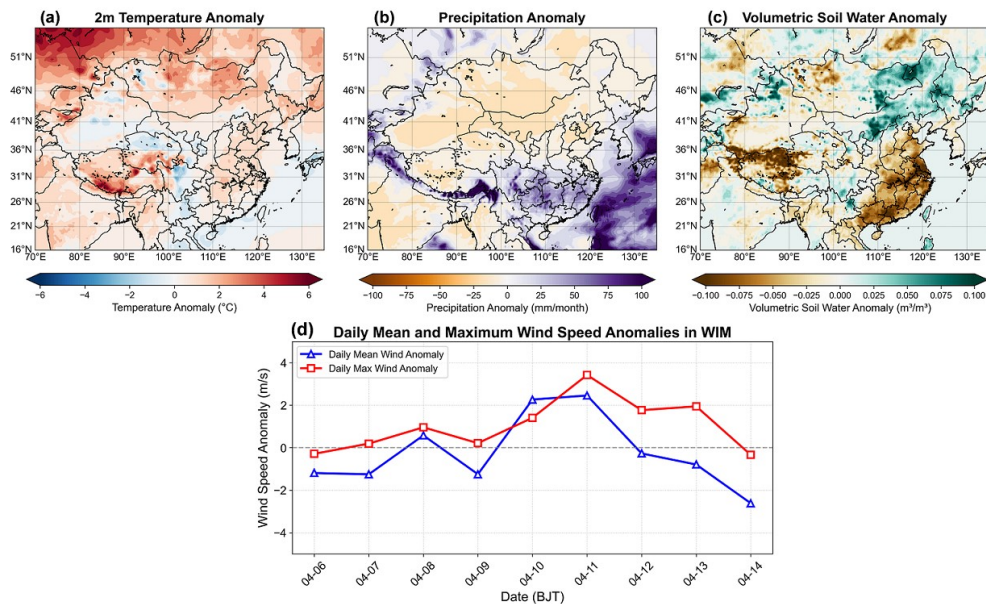


Figure 8. Spatial distribution of mean anomalies for temperature ($^{\circ}\text{C}$), total precipitation (mm) and top-layer volumetric soil water (m^3/m^3) over China from January 1, 2025 to April 13, 2025 BJT relative to the 30-year baseline of 1995-2024 (a-c). Daily anomaly time series of daily mean and maximum surface wind speed (m/s) from April 09 to 14, 2025 BJT (Relative to 30-year baseline: 1995-2024) in WIM (d). All data are from the ERA5 reanalysis.

4.3.2 Comparison with historical severe dust storms

In order to further explore the dynamical and physical processes during this dust event, the historical dust events in northern China since 2000 are collected and compiled, and the two mostA dust storm is a severe aeolian weather phenomenon characterized by strong winds lifting large amounts of dust from the surface into the air, resulting in exceptionally turbid atmospheric conditions and horizontal visibility reduced to less than one kilometer. Based on meteorological observation data, the China Meteorological Administration has recognized the dust events occurring in April 2023 and March 2021 as two severe dust storm episodes. The 2021 case represents peak intensity and lateral spread, yet stalled in central-eastern China, whereas the 2025 event achieved pronounced southward transport. The 2023 case showed southward potential but failed to penetrate deeply, unlike the 2025 event, which crossed the Yangtze River despite precipitation (Yu et al., 2023; Yang et al., 2025). In order to further explore the dynamical and physical processes during this dust event, the two severe dust events (one on March 14, 2021, and the other on April 9, 2023) are selected for comparison. Similar to the 2025 event, these historical events originated from source areas including WIM region and were primarily driven by Mongolian cyclones (Mikalai et al., 2022; Mikalai et al., 2024). However, neither historical event reached Hainan Province (Figure S3S4). By looking into the meteorological condition and soil moisture, ~~to~~we compare and understand the differences in the dust emission, transport, and scavenging processes for the selected dust events.

To compare the intensity of the three dust events occurring in March 2021, April 2023, and April 2025, the regional averages of ~~both~~ daily maximum PM_{10} concentrations in the WIM region during these events were analysed. As shown in

Figure 9, the peak regional average daily maximum PM₁₀ concentrations for the 2021, 2023, and 2025 dust events were 749 μg/m³, 708 μg/m³, and 841 μg/m³, respectively. This indicates that all three events were relatively intense, with no significant difference in their outbreak intensity. The meteorological conditions including precipitation, wind speed and surface temperature, as well as soil moisture in the dust source regions strongly influence dust emissions (Ishizuka et al., 2008; Kim et al., 2015; Yang et al., 2019). To further investigate the causes of the three dust events, Figure 10 shows the time series of daily anomaly for precipitation, volumetric soil water, and surface temperature during the four months preceding the three dust events, as well as the daily mean anomalies of maximum wind speed for the five days before and after the dust events in the WIM region. Our analysis indicates that during the four months prior to the dust events and the month when the dust event occurred, the precipitation and soil moisture were well correlated. The monthly total precipitation anomaly and volumetric soil water anomaly in 2025 were close to zero, whereas those in 2021 and 2023 were predominantly negative. The surface temperature in 2025 was higher than during both historical events (approximately about 8 K higher than the 30-year mean, while the positive anomalies in 2021 and 4 K higher than in 2023). Precipitation levels during the four months preceding the three events were relatively similar. However, in the month when the dust events occurred, the precipitation in 2025 (approximately 10 mm) was significantly, though present, were lower than that of 2025. In addition, the daily maximum wind speed anomaly during the 2025 dust event peaked at about +4 m/s on the day of the dust outbreak (April 11, 2025), which was higher than the peaks in the two historical events (30 mm about +3 m/s in 2023 and 20 mm slightly above 0 m/s in 2021). Correspondingly, Although the long-term precipitation and soil moisture in before the month of the 2025 dust event (approximately 0.1 m³/m³) was significantly lower than that during the months of the two historical events (approximately 0.15 m³/m³). Furthermore, on the day of the dust outbreak, the daily mean wind speed 2025 event did not show conditions particularly favourable for dust emission, the persistent high temperature combined with a short-term strong wind event provided favourable conditions for the outbreak of the 2025 dust event (approximately 3.5 m/s) was significantly higher than that of the two historical events (approximately 2 m/s)-storm.

设置了格式: 字体颜色: 黑色

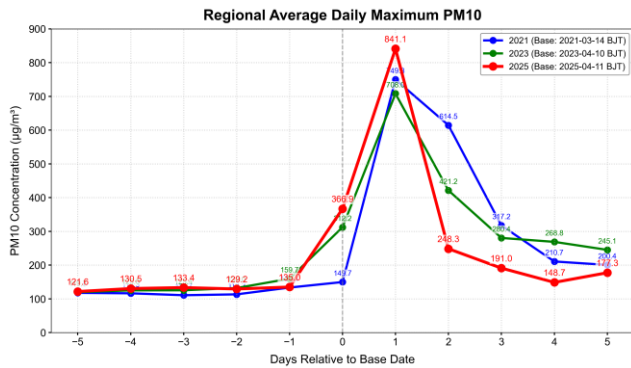


Figure 9. The temporal evolution of regionally averaged PM₁₀ concentrations (daily maximum, unit: μg/m³) from monitoring stations within the WIM region (38°N-43°N, 98°E-110°E), during dust events in March 2021, April 2023, and April 2025. Data are plotted relative to the dust event onset date (day 0) for each year, with ±5-day analysis windows. Gray dashed line marks the dust onset day (day 0).

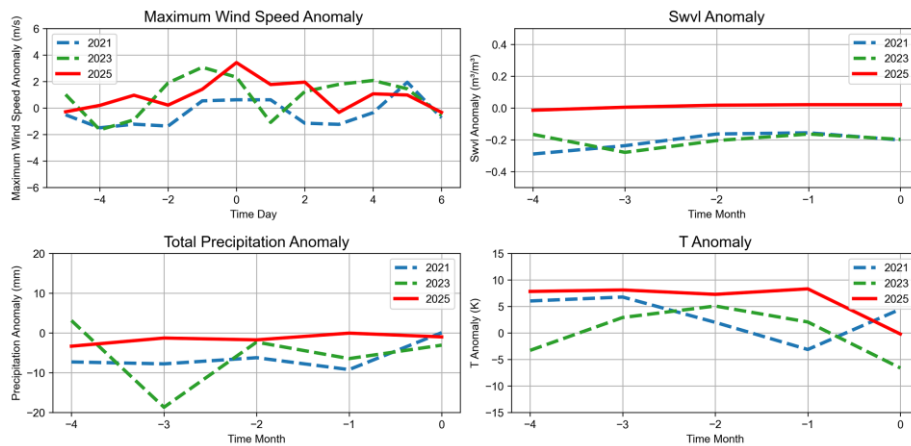


Figure 10. Daily anomaly time series (5 days pre- and post-dust event onset) of surface maximum wind speed (m/s) in WIM (38°N-43°N, 98°E-110°E). Monthly anomaly time series (4 months pre-dust event onset) of key parameters in WIM (38°N-43°N, 98°E-110°E), including top-layer volumetric soil water (Swvl, unit: m³/m³), total precipitation (mm), surface temperature (T, unit: K). All data are from the ERA5 reanalysis.

Figure 11 presents the spatial-temporal variations of the PM₁₀ mass concentration, wind field, and precipitation during three dust event periods. It is clearly shown that although strong dust emissions occurred in WIM for three dust events (first row-second rows), the magnitude and pathway of dust transport exhibits quite different behaviour (second-fourth-third-fifth rows). For the case in March 2021, strong northerly winds pushed dust particles to central-eastern China on Mar 15, and then remain stagnant and had no further southern-ward transport until March 16 due to quite weak wind speed. For the case in April 2023, the wind speed was apparently stronger than that in 2021 case, so dust particles could be transported to eastern China and even northeast China. The lack of sustained strong northerly winds over the North China Plain on April 11-12 limited the southward spread of dust to southern China. Different from two above cases, dust aerosols in April 2025 reached the Yangtze River Basin, and sustained strong northerly winds exceeding 8 m/s provided sufficient momentum and make dust particles crossed the Yangtze River and further transport southward to the South China Sea. Wet scavenging of dust particles are negligible due to very limited precipitation for the 2021 and 2023 cases. In the April 2025 dust event, a distinct rainbelt was observed over eastern China was observed during the 2025 case, but dust southward transport was not affected wet scavenging due to precipitation since. However, the dust aerosols consistently remained behind the rainbelt. Therefore, the reason why the dust storm during April 2025 can be transported to the most southern China is mostly attributed to favourable meteorological conditions, i.e., and their southward transport was largely unaffected by wet scavenging. In contrast to the two historical cases, strong and persistent northerly winds, for during this event enhanced both dust emission and long-range transport, and combined. Consequently, with weak limited wet scavenging by precipitation, the dust storm was able to reach the far south of China primarily due to the strong wind-driven transport.

To investigate the causes of the persistent strong northerly winds during the 2025 event, a comparative analysis of the dynamic mechanisms was conducted in relation to the atmospheric circulation patterns. Figures 5 and S5 illustrate the characteristics of atmospheric circulation during the 2025, 2021, and 2023 events. The analysis shows that the Mongolian cyclone was a key influencing system in all three events, but its evolution and configuration with the Siberian High differed significantly, leading to variations in the intensity and persistence of the northerly winds.

设置了格式: 字体颜色: 自动设置
 设置了格式: 字体颜色: 自动设置
 设置了格式: 字体颜色: 自动设置
 设置了格式: 字体颜色: 自动设置

设置了格式: 字体颜色: 自动设置
 设置了格式: 字体颜色: 自动设置
 设置了格式: 字体颜色: 自动设置
 设置了格式: 字体颜色: 自动设置
 设置了格式: 字体颜色: 蓝色

During the 2023 event, the Mongolian cyclone occurred in northern China and dominated the process, while the Siberian High played a relatively weaker role. Strong northerly winds were mainly observed on April 10 and 11, 2023, coinciding with the formation and development of the Mongolian cyclone. In both the 2021 and 2025 events, the combined influence of the Mongolian cyclone and the Siberian High was evident. During periods of strong northerly winds, the synergistic interaction between the two systems was pronounced (both were in the developmental stage with closely positioned pressure centers). However, differences existed in the duration and location of the Mongolian cyclone. In the 2021 event, the Mongolian cyclone dissipated relatively quickly (lasting only two days, March 14-15, 2021) and was primarily located in northern China. In the 2025 event, the Mongolian cyclone formed on the day of the dust outbreak and gradually intensified, with its location approximately 5 degrees of latitude farther south compared to the other two events. In summary, the persistent and strong northerly winds during the 2025 event were primarily driven by the sustained synergistic interaction between the intense Siberian High and the Mongolian cyclone, coupled with the southerly displacement of the cyclone's position. These factors collectively provided the sustained and robust dynamic conditions essential for the long-range southward transport of dust.

375

380

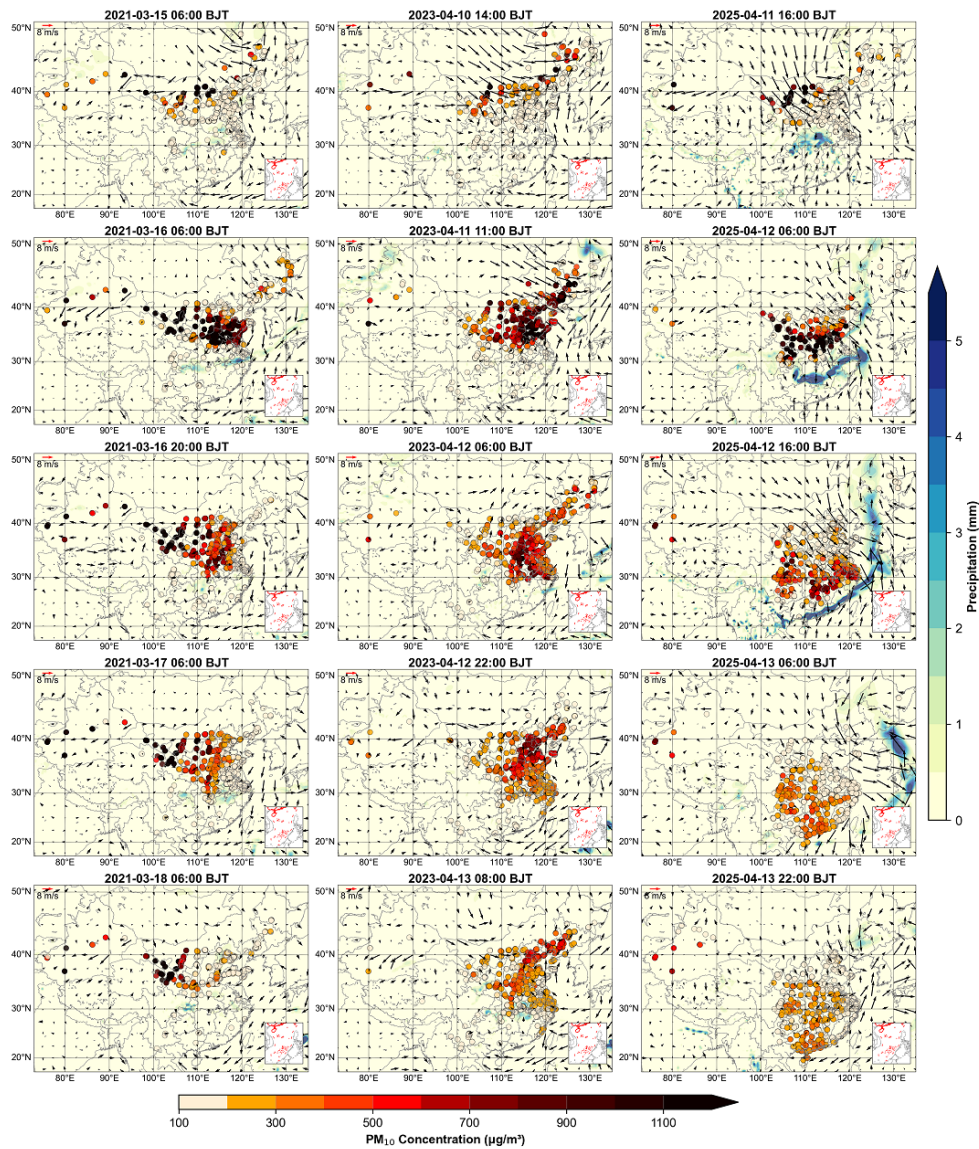


Figure 11. Spatial distribution of hourly accumulated precipitation (mm), surface wind fields, and PM₁₀ concentrations (µg/m³) over China during dust events: March 2021, April 2023, and April 2025. Precipitation is shown as color-filled maps, with PM₁₀ displayed as solid circles. Hourly accumulated precipitation and surface wind fields data are sourced from ERA5, while hourly PM₁₀ concentration data are obtained from surface monitoring stations.

385

5 Summary and Conclusion

We analyze the basic characteristics of the outbreak and transport processes of a severe dust event that occurred in northern China on April 11, 2025, especially focus on its emission and vertical transport, and then investigate the dust emission mechanisms and transport pathways involved by comparing meteorological conditions against the 30-year climatological average and contrasting the event with two ~~typical~~ ~~severe~~ historical dust storms.

Starting from 17:00 Beijing Time on April 11, 2025, a dust storm occurred in WIM accompanied by strong northerly winds exceeding 8 m/s, and the hourly PM₁₀ concentration surged to over 1900 µg/m³. The GEOS-Chem model simulations indicate that the emission flux exceeded 400 µg/m²/s, and vertical transport reached 3.6 km. ~~Usually, dust emissions in source regions can reach approximately 500 µg/m²/s (Zhao et al., 2020), and dust aerosols can be vertically transported to about 3 km above the source region (Tsai et al., 2008).~~ Under the synergistic effect of the Siberian cold high-pressure system and the Mongolian cyclone, WIM remained within the dry-cold advection zone west of the cyclone. The combination of low relative humidity and wind speeds over 10 m/s provided favorable dynamic conditions for dust emission. Furthermore, strong northerly winds in the WIM region guided the dust toward the North China Plain. ~~The southward-moving dry-cold air mass gradually dominated the middle and lower reaches of the Yangtze River, creating favorable conditions for dust transport to Hainan.~~ The dust reached the Yangtze River Basin on April 12 and arrived at Hainan Island by April 13, where observed PM₁₀ exceeded 200 µg/m³ and simulated dust concentration surpassed 20 µg/m³. ~~During this event, dust aerosols originating from the WIM region were transported an exceptionally long distance to Hainan Province, affecting most areas marking a phenomenon that has not been clearly documented in observational records of northern, central, and southern China East Asian dust events in recent years.~~

The comparisons of meteorological conditions during this dust event against the 30-year climatological mean from ERA5 reanalysis data indicate that the dust source region (WIM) exhibited persistent high-temperature and drought conditions during the four months preceding the event, i.e. air temperature was approximately +2 °C above the baseline, precipitation was about 25 mm below normal, and volumetric soil water content was approximately 0.02 m³/m³ lower than the baseline. Short-term wind field analysis before dust emission showed a positive ~~average~~ wind speed anomaly of approximately +2 m/s on the day before the outbreak (April 10), which peaked on the dust event day (April 11). ~~Besides, maximum wind speed anomaly was approximately +4 m/s on April 11.~~ Prolonged high temperature and drought led to desiccated and loosened surface soil, providing ample source material for dust emission, while the strong winds preceding the event supplied crucial dynamic conditions. The synergistic interaction of these factors constituted the core triggering mechanism for this dust event.

To further discuss the reasons causing the long-range transport during this dust event, we selected two ~~typical~~ ~~severe~~ historical dust events in northern China (March 14, 2021, and April 9, 2023) for comparative analysis. Although all three events originated from the same source regions including WIM and were primarily driven by Mongolian cyclones, the 2025 event achieved ultra-long-range transport to Hainan, while the historical events did not affect southern China. Comparison of the daily maximum PM₁₀ concentrations in the WIM region revealed values of 749 µg/m³ (2021) and 708 µg/m³ (2023), whereas the 2025 event reached 841 µg/m³, indicating slightly higher intensity. Analysis of dust emission conditions for the three events based on ERA5 reanalysis data ~~showed that the volumetric soil water content during the month of the 2025 event (approximately 0.1 m³/m³) was significantly lower than during the months of the historical events. This is primarily attributed to the much lower~~ ~~indicates a clear correspondence between~~ precipitation in April 2025 (near 10 mm) compared to April 2023 (over 30 mm) and March 2021 (about 20 mm), while temperature, humidity, and precipitation anomalies over the preceding four months showed no significant differences among the three events. ~~Meanwhile soil moisture, with anomaly values for both in 2025 close to zero, whereas distinct negative anomalies are observed in the historical events of 2023 and 2021. The surface temperature in 2025 was approximately 8 K higher than the 30-year mean, significantly exceeding the anomalies in 2021 and~~

设置了格式: 字体: +西文正文 (Calibri), 五号, 字体颜色: 自动设置

430 ~~2023. In addition, the regional average daily maximum wind speed anomaly on the day of the 2025 event (close to 4 m/s) was significantly markedly stronger than that during the two historical events. This indicates that the nearly month-While long-dry-term moisture conditions before the 2025 event reduced soil moisture, effectively providing a dust source, while they were not particularly conducive, the combination of persistent high temperatures and a short-term strong winds on the event day provided the key lifting-forewind event generated conditions that favored dust emission in 2025.~~

435 To look into long-range transport conditions, the PM₁₀ concentrations, and wind fields and precipitation patterns during the emission and transport periods of the three dust events were compared. Our study found that both the 2021 and 2023 events were limited by the lack of persistent strong northerly winds along their transport paths (over North and Central China), ultimately preventing long-range transport to southern China. In contrast, the 2025 event exhibited two key features: (1) dust aerosols consistently remained behind the rainband and moved southward synchronously with it, effectively avoiding wet scavenging; and (2) sustained strong northerly winds exceeding 8 m/s continuously pushed the dust over the Yangtze River Basin, enabling ultra-long-range transport to Hainan. ~~The formation of these two key features is primarily attributable to the unique characteristics of the driving "Mongolian Cyclone-Siberian High" coupling during this event, particularly in terms of its intensity configuration (prolonged duration) and spatial configuration (southerly-displaced position of the cyclone).~~

440 In summary, this study demonstrates that ~~under the sustained interaction of the "Mongolian Cyclone-Siberian High" system, coupled with the southerly displacement of the Mongolian cyclone,~~ the southward movement of a dry-cold air mass driven by persistent strong northerly winds resulted in coordinated southward movement of dust and the rainband, which collectively facilitated the stable long-range transport of dust in the 2025 event. These results highlight the critical leading role of airflow transport under specific synoptic conditions.

Acknowledgements

450 This research has been supported by the National Natural Science Foundation of China (grant nos. 42575082, 42061134009 and 41975002). We are thankful to the GEOS-Chem Support Team for their management and maintenance of the GEOS-Chem model. We acknowledge the use of ERA5 reanalysis data provided by the European Centre for Medium-Range Weather Forecasts (ECMWF). We are also grateful to NASA, the Chinese Ministry of Environmental Protection and the Chinese National Meteorological Center for providing the MODIS datasets, surface PM10 observations and meteorological measurements respectively.

455 Author contributions

PZ was responsible for data analysis and drafted the manuscript. XM participated in the conceptualization of the study, data analysis, and article writing. RT contributed to the model simulations and, together with JZ, TY, and YK, assisted in the manuscript preparation.

Competing interests

460 The authors declare that they have no conflict of interest.

Reference:

- An L, Che H, Xue M, et al. Temporal and spatial variations in sand and dust storm events in East Asia from 2007 to 2016: Relationships with surface conditions and climate change[J]. Science of The Total Environment, 2018, 633: 452-462.
- Attiya A A, Jones B G. Climatology of Iraqi dust events during 1980–2015[J]. SN Applied Sciences, 2020, 2(5): 845.

设置了格式: 字体: +西文正文 (Calibri), 五号, 字体颜色: 自动设置

- 465 Bao C, Yong M, ** E, et al. Regional spatial and temporal variation characteristics of dust in East Asia[J]. *Chin. J. Geogr. Res.*, 2021, 40: 14.
- Borjigin A, Bueh C, Yong M, et al. Cross-border sand and dust storms between Mongolia and Northern China in spring and their driving weather systems[J]. *Remote Sensing*, 2024, 16(12): 2164.
- Bergametti G, Forêt G. Dust deposition[M]/Mineral dust: A key player in the earth system. Dordrecht: Springer Netherlands, 2014: 179-200.
- 470 Chaibou A A S, Ma X, Kumar K R, et al. Evaluation of dust extinction and vertical profiles simulated by WRF-Chem with CALIPSO and AERONET over North Africa[J]. *Journal of Atmospheric and Solar-Terrestrial Physics*, 2020, 199: 105213.
- Chen, Yu, et al. "Where is the Dust Source of 2023 Several Severe Dust Events in China?." *Bulletin of the American Meteorological Society* 105.11 (2024): E2085-E2096.
- 475 Chen, G. T.-J., and H.-J. Chen (1987), Study on large-scale features of duststorm systems in East Asia, *Meteor. Res.*, 10(1), 57–79.
- Chen S Y, Huang J P, Li J X, et al. Comparison of dust emissions, transport, and deposition between the Taklimakan Desert and Gobi Desert from 2007 to 2011[J]. *Science China Earth Sciences*, 2017, 60(7): 1338-1355.
- Chepil W S. Influence of moisture on erodibility of soil by wind[J]. *Soil Science Society of America Journal*, 1956, 20(2): 288-292.
- Field J P, Belnap J, Breshears D, et al. The ecology of dust[J]. *Frontiers in Ecology and the Environment*, 2010, 8(8): 423-430.
- 480 Fu et al. "Source, transport and impacts of a heavy dust event in the Yangtze River Delta, China, in 2011." *Atmospheric Chemistry and Physics* 14.3 (2014): 1239-1254.
- Farmer D K, Boedicker E K, DeBolt H M. Dry deposition of atmospheric aerosols: Approaches, observations, and mechanisms[J]. *Annual review of physical chemistry*, 2021, 72(1): 375-397.
- Guan Q, Sun X, Yang J, et al. Dust storms in northern China: Long-term spatiotemporal characteristics and climate controls[J]. *Journal of Climate*, 2017, 30(17): 6683-6700.
- 485 Gao H, Qi J, Shi J, et al. Long-range Transport of Asian Dust and Its Effects on Ocean Ecosystem [J]. *Advances in earth science*, 2009, 24(1): 1.
- Gassó S, Grassian V H, Miller R L. Interactions between mineral dust, climate, and ocean ecosystems[J]. *Elements*, 2010, 6(4): 247-252.
- Griffin D W, Kellogg C A. Dust storms and their impact on ocean and human health: dust in Earth's atmosphere[J]. *EcoHealth*, 2004, 1(3): 284-295.
- 490 Guo J, Lou M, Miao Y, et al. Trans-Pacific transport of dust aerosols from East Asia: Insights gained from multiple observations and modeling[J]. *Environmental Pollution*, 2017, 230: 1030-1039.
- Gavrouzou, Maria, et al. "A global climatology of dust aerosols based on satellite data: Spatial, seasonal and inter-annual patterns over the period 2005–2019." *Remote Sensing* 13.3 (2021): 359.
- 495 Huang J, Lin B, Minnis P, et al. Satellite - based assessment of possible dust aerosols semi - direct effect on cloud water path over East Asia[J]. *Geophysical Research Letters*, 2006, 33(19).
- Huang J, Wang T, Wang W, et al. Climate effects of dust aerosols over East Asian arid and semiarid regions[J]. *Journal of Geophysical Research: Atmospheres*, 2014, 119(19): 11,398-11,416.
- 500 Hussein T, Karppinen A, Kukkonen J, et al. Meteorological dependence of size-fractionated number concentrations of urban aerosol particles[J]. *Atmospheric Environment*, 2006, 40(8): 1427-1440.
- Husar R B, Tratt D M, Schichtel B A, et al. Asian dust events of April 1998[J]. *Journal of Geophysical Research: Atmospheres*, 2001, 106(D16): 18317-18330.
- Hu Y Q, Chen J B, Zuo H C. Theorem of turbulent intensity and macroscopic mechanism of the turbulence development[J]. *Science in China Series D: Earth Sciences*, 2007, 50(5): 789-800.
- 505 Iwasaka Y, Minoura H, Nagaya K. The transport and spacial scale of Asian dust-storm clouds: a case study of the dust-storm event of April 1979[J]. *Tellus B: Chemical and Physical Meteorology*, 1983, 35(3): 189-196.

- Idso S B. Dust storms[J]. *Scientific American*, 1976, 235(4): 108-115.
- Kim J. Transport routes and source regions of Asian dust observed in Korea during the past 40 years (1965–2004) [J]. *Atmospheric Environment*, 2008, 42(19): 4778-4789.
- 510 Kim, Sang-Woo, et al. "Asian dust event observed in Seoul, Korea, during 29–31 May 2008: Analysis of transport and vertical distribution of dust particles from lidar and surface measurements." *Science of the Total Environment* 408.7 (2010): 1707-1718.
- Knippertz P, Fink A H. Synoptic and dynamic aspects of an extreme springtime Saharan dust outbreak[J]. *Quarterly Journal of the Royal Meteorological Society: A journal of the atmospheric sciences, applied meteorology and physical oceanography*, 2006, 132(617): 1153-1177.
- 515 Kai Z, Huiwang G. The characteristics of Asian-dust storms during 2000–2002: From the source to the sea[J]. *Atmospheric Environment*, 2007, 41(39): 9136-9145.
- Liang, Lin, et al. "Emission, transport, deposition, chemical and radiative impacts of mineral dust during severe dust storm periods in March 2021 over East Asia." *Science of the Total Environment* 852 (2022): 158459.
- Lu H, Shao Y. A new model for dust emission by saltation bombardment[J]. *Journal of Geophysical Research: Atmospheres*, 1999, 104(D14): 16827-16842.
- 520 Lee E H, Sohn B J. Recent increasing trend in dust frequency over Mongolia and Inner Mongolia regions and its association with climate and surface condition change[J]. *Atmospheric Environment*, 2011, 45(27): 4611-4616.
- Liu Z, Omar A, Vaughan M, et al. CALIPSO lidar observations of the optical properties of Saharan dust: A case study of long-range transport[J]. *Journal of Geophysical Research: Atmospheres*, 2008, 113(D7).
- 525 Liu Y, Liu R. Climatology of dust storms in northern China and Mongolia: Results from MODIS observations during 2000–2010[J]. *Journal of Geographical Sciences*, 2015, 25(11): 1298-1306.
- Liu L, Wang Z, Che H, et al. Climate factors influencing springtime dust activities over Northern East Asia in 2021 and 2023[J]. *Atmospheric Research*, 2024, 303: 107342.
- Liu T H, Tsai F, Hsu S C, et al. Southeastward transport of Asian dust: Source, transport and its contributions to Taiwan[J]. *Atmospheric Environment*, 2009, 43(2): 458-467.
- 530 Littmann T. Rainfall, temperature and dust storm anomalies in the African Sahel[J]. *Geographical Journal*, 1991: 136-160.
- Li J, Hao X, Liao H, et al. Predominant type of dust storms that influences air quality over northern China and future projections[J]. *Earth's Future*, 2022, 10(6): e2022EF002649.
- Miri A, Middleton N. Long-term impacts of dust storms on transport systems in south-eastern Iran[J]. *Natural Hazards*, 2022, 114(1): 291-312.
- 535 Ma X, Von Salzen K. Dynamics of the sulphate aerosol size distribution on a global scale[J]. *Journal of Geophysical Research: Atmospheres*, 2006, 111(D8).
- Ma X, Bartlett K, Harmon K, et al. Comparison of AOD between CALIPSO and MODIS: significant differences over major dust and biomass burning regions[J]. *Atmospheric Measurement Techniques*, 2013, 6(9): 2391-2401.
- 540 Munkhtsetseg E, Shinoda M, Gillies J A, et al. Relationships between soil moisture and dust emissions in a bare sandy soil of Mongolia[J]. *Particuology*, 2016, 28: 131-137.
- McKendry, I. G., J. P. Hacker, R. Stull, S. Sakiyama, D. Mignacce, and K. Reid (2001), Long-range transport of Asian dust to the lower Fraser Valley, British Columbia, Canada, *J. Geophys. Res.*, 106(D16), 18,361–18,370.
- Mikalai F. Characteristics of the severe March 2021 Gobi Desert dust storm and its impact on air pollution in China[J]. *Chemosphere*, 2022,287(P3):132219-132219.
- 545 Mikalai F, P. M P, Lifeng Z, et al. An analysis of air pollution associated with the 2023 sand and dust storms over China: Aerosol properties and PM10 variability[J]. *Geoscience Frontiers*,2024,15(2):101762-.
- Park S, Allen R J. Understanding influences of convective transport and removal processes on aerosol vertical distribution[J]. *Geophysical*

- Research Letters, 2015, 42(23): 10,438-10,444.
- 550 Park S U, Choe A, Park M S. Estimates of Asian dust deposition over the Asian region by using ADAM2 in 2007[J]. Science of the total environment, 2010, 408(11): 2347-2356.
- Pryor S C, Barthelme R J. Particle dry deposition to water surfaces: processes and consequences[J]. Marine Pollution Bulletin, 2000, 41(1-6): 220-231.
- Qian W, Quan L, Shi S. Variations of the dust storm in China and its climatic control[J]. Journal of climate, 2002, 15(10): 1216-1229.
- 555 Ravi S, D'Odorico P, Over T M, et al. On the effect of air humidity on soil susceptibility to wind erosion: The case of air - dry soils[J]. Geophysical Research Letters, 2004, 31(9).
- Richter D, Chamecki M. Inertial effects on the vertical transport of suspended particles in a turbulent boundary layer[J]. Boundary-layer meteorology, 2018, 167(2): 235-256.
- Roth M. Review of atmospheric turbulence over cities[J]. Quarterly Journal of the Royal Meteorological Society, 2000, 126(564): 941-990.
- 560 Shao Y, Zhang J, Ishizuka M, et al. Dependency of particle size distribution at dust emission on friction velocity and atmospheric boundary-layer stability[J]. Atmospheric Chemistry and Physics Discussions, 2020, 2020: 1-14.
- Seinfeld, J. H., Carmichael, G. R., Arimoto, R., Conant, W. C., Brechtel, F. J., Bates, T. S., et al. (2004). ACE-ASIA: Regional Climatic and Atmospheric Chemical Effects of Asian Dust and Pollution. Bulletin of the American Meteorological Society, 85(3), 367–380.
- Sun J, Zhang M, Liu T. Spatial and temporal characteristics of dust storms in China and its surrounding regions, 1960–1999: Relations to source area and climate[J]. Journal of Geophysical Research: Atmospheres, 2001, 106(D10): 10325-10333.
- 565 Siyu C, Dan Z, Jianping H, et al. Mongolia Contributed More than 42% of the Dust Concentrations in Northern China in March and April 2023[J]. Advances in Atmospheric Sciences, 2023, 40(9): 1549-1557.
- Song P, Fei J, Li C, et al. Simulation of an Asian Dust Storm Event in May 2017[J]. Atmosphere, 2019, 10(3): 135.
- Tian R, Ma X, Zhao J. A revised mineral dust emission scheme in GEOS-Chem: improvements in dust simulations over China[J]. Atmospheric Chemistry and Physics Discussions, 2020, 2020: 1-24.
- 570 Twomey, S. (1977). The Influence of Pollution on the Shortwave Albedo of Clouds. Journal of the Atmospheric Sciences, 34(7), 1149–1152. [https://doi.org/10.1175/1520-0469\(1977\)034%3C1149:tiopot%3E2.0.co;2](https://doi.org/10.1175/1520-0469(1977)034%3C1149:tiopot%3E2.0.co;2)
- Tang Y, et al. The improved parameterization scheme of dust emission for dust devils in northern China and numerical simulation of its radiative effects [D]. Nanjing University of Information Science and Technology, 2018.
- 575 Tan S C, Shi G Y, Wang H. Long-range transport of spring dust storms in Inner Mongolia and impact on the China seas[J]. Atmospheric environment, 2012, 46: 299-308.
- Tian Y, Pan X, Jing Y, et al. East Asia dust storms in spring 2021: Transport mechanisms and impacts on China[J]. Atmospheric Research, 2023, 290
- Tegen I, Harrison S P, Kohfeld K, et al. Impact of vegetation and preferential source areas on global dust aerosol: Results from a model study[J]. Journal of Geophysical Research: Atmospheres, 2002, 107(D21): AAC 14-1-AAC 14-27.
- 580 Takemi T, Scino N. Dust storms and cyclone tracks over the arid regions in east Asia in spring[J]. Journal of Geophysical Research: Atmospheres, 2005, 110(D18).
- Tsai F, Chen G T J, Liu T H, et al. Characterizing the transport pathways of Asian dust[J]. Journal of geophysical research: atmospheres, 2008, 113(D17).
- 585 Tsendendamba P, Dulam J, Baba K, et al. Northeast Asian dust transport: A case study of a dust storm event from 28 March to 2 April 2012[J]. Atmosphere, 2019, 10(2): 69.
- Uno I, Yumimoto K, Shimizu A, et al. 3D structure of Asian dust transport revealed by CALIPSO lidar and a 4DVAR dust model[J]. Geophysical Research Letters, 2008, 35(6).
- Wang X, Oenema O, Hoogmoed W B, et al. Dust storm erosion and its impact on soil carbon and nitrogen losses in northern China[J]. Catena, 2006, 66(3): 221-227.
- 590

- Wang X, Huang J, Ji M, et al. Variability of East Asia dust events and their long-term trend[J]. *Atmospheric Environment*, 2008, 42(13): 3156-3165.
- Wang X, Dong Z, Zhang J, et al. Modern dust storms in China: an overview[J]. *Journal of Arid Environments*, 2004, 58(4): 559-574.
- Wang X, Liu J, Che H, et al. Spatial and temporal evolution of natural and anthropogenic dust events over northern China[J]. *Scientific Reports*, 2018, 8(1): 2141.
- 595 Wang S, Yu Y, Zhang X, et al. Weakened dust activity over China and Mongolia from 2001 to 2020 associated with climate change and land-use management[J]. *Environmental Research Letters*, 2021, 16(12): 124056.
- Wang L P. On the dispersion of heavy particles by turbulent motion[M]. Washington State University, 1990.
- Wang W, Samat A, Abuduwaili J, et al. Temporal characterization of sand and dust storm activity and its climatic and terrestrial drivers in the Aral Sea region[J]. *Atmospheric Research*, 2022, 275: 106242.
- 600 Xiao F, Wong M S, Lee K H, et al. Retrieval of dust storm aerosols using an integrated Neural Network model[J]. *Computers & Geosciences*, 2015, 85: 104-114.
- Xiong J, Zhao T, Bai Y, et al. Climate characteristics of dust aerosol and its transport in major global dust source regions[J]. *Journal of Atmospheric and Solar-Terrestrial Physics*, 2020, 209: 105415.
- 605 Xu X, Levy J K, Zhaohui L, et al. An investigation of sand-dust storm events and land surface characteristics in China using NOAA NDVI data[J]. *Global and Planetary Change*, 2006, 52(1-4): 182-196.
- Yang Y Q, Hou Q, Zhou C H, et al. Sand/dust storm processes in Northeast Asia and associated large-scale circulations[J]. *Atmospheric Chemistry and Physics*, 2008, 8(1): 25-33.
- Yang Y Q, Hou Q, Zhou C H, et al. Sand/dust storms over Northeast Asia and associated large-scale circulations in spring 2006[J]. *Atmospheric Chemistry and Physics Discussions*, 2007, 7(3): 9259-9281.
- 610 Yu T, Xiaole P, Yujie J, et al. East Asia dust storms in spring 2021: Transport mechanisms and impacts on China[J]. *Atmospheric Research*, 2023, 290: 106773.
- Yong M, Shinoda M, Nandintsetseg B, et al. Impacts of land surface conditions and land use on dust events in the inner Mongolian grasslands, China[J]. *Frontiers in Ecology and Evolution*, 2021, 9: 664900.
- 615 Zhang, Renjian, et al. "Ground observations of a strong dust storm in Bei**g in March 2002." *Journal of Geophysical Research: Atmospheres* 110.D18 (2005).
- Zhang X Y, Arimoto R, An Z S. Glacial and interglacial patterns for Asian dust transport[J]. *Quaternary Science Reviews*, 1999, 18(6): 811-819.
- Zhao, Jianqi, et al. "Dust emission and transport in Northwest China: WRF-Chem simulation and comparisons with multi-sensor observations." *Atmospheric Research* 241 (2020): 104978.
- 620 Zhao, Q., et al. "Dust storms come to Central and Southwestern China, too: implications from a major dust event in Chongqing." *Atmospheric Chemistry and Physics* 10.6 (2010): 2615-2630.
- Zobeck T M. Soil properties affecting wind erosion[J]. *Journal of Soil and water conservation*, 1991, 46(2): 112-118.
- Zhang R, Han Z, Wang M, et al. Dust storm weather in China: New characteristics and origins[J]. *Quaternary Sciences*, 2002, 22(4): 374-380.
- 625 Zhang L, Zhang H, Li Q, et al. Vertical dispersion mechanism of long-range transported dust in Beijing: Effects of atmospheric turbulence[J]. *Atmospheric Research*, 2022, 269: 106033.
- Zhu Q, Liu Y. The dominant factor in extreme dust events over the Gobi Desert is shifting from extreme winds to extreme droughts[J]. *npj Climate and Atmospheric Science*, 2024, 7(1): 141.
- 630 Zhao T L, Gong S L, Zhang X Y, et al. Modeled size - segregated wet and dry deposition budgets of soil dust aerosol during ACE - Asia 2001: Implications for trans - Pacific transport[J]. *Journal of Geophysical Research: Atmospheres*, 2003, 108(D23).
- Zhao C, Dabu X, Li Y. Relationship between climatic factors and dust storm frequency in Inner Mongolia of China[J]. *Geophysical research*

letters, 2004, 31(1).

635

Zhao T L, Gong S L, Zhang X Y, et al. Asian dust storm influence on North American ambient PM levels: observational evidence and controlling factors[J]. *Atmospheric Chemistry and Physics*, 2008, 8(10): 2717-2728.

Zou X K, Zhai P M. Relationship between vegetation coverage and spring dust storms over northern China[J]. *Journal of Geophysical Research: Atmospheres*, 2004, 109(D3).

Zannetti P. Dry and wet deposition[M]//*Air Pollution Modeling: Theories, Computational Methods and Available Software*. Boston, MA: Springer US, 1990: 249-262.